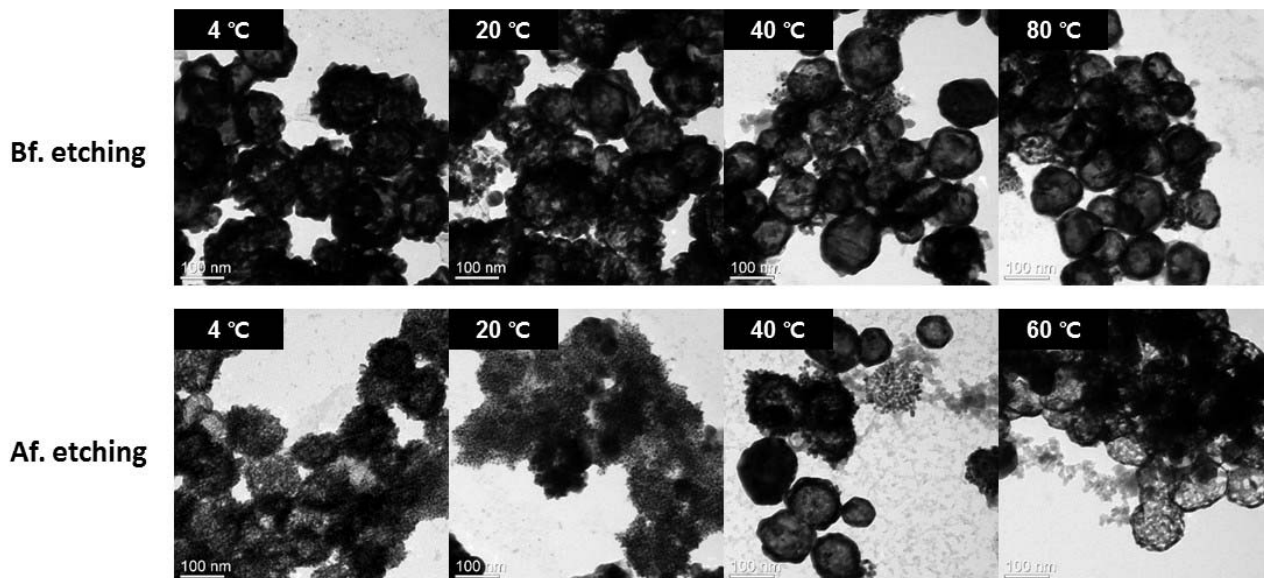
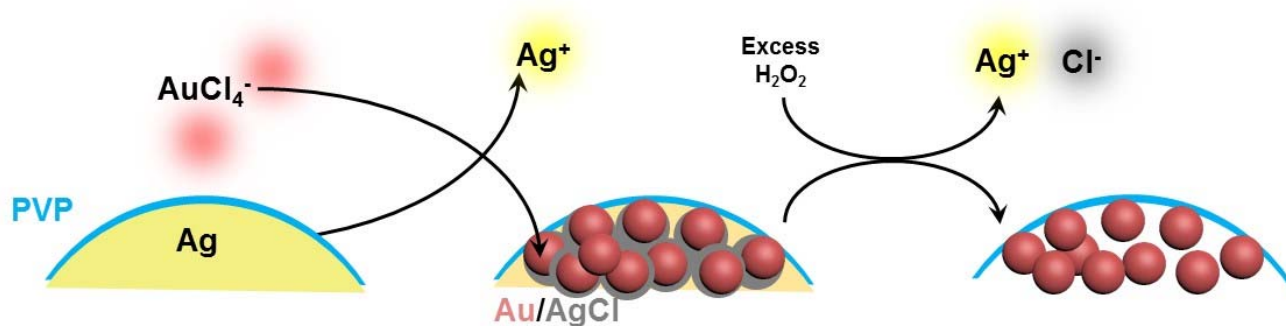


# Supporting Information

## Spherically-Clustered Porous Au-Ag Alloy Nanoparticle Prepared by Partial Inhibition of Galvanic Replacement and Its Application for Efficient Multi-Modal Therapy

*Hongje Jang and Dal-Hee Min\**

Department of Chemistry, Center for RNA Research, Institute for Basic Sciences (IBS),  
Seoul National University, Seoul, 151-747, Republic of Korea



**Figure S1.** Galvanic replacement of precursor PVP-AgNP under the temperature mediated galvanic replacement reaction inhibition. (a) The assumed mechanism for the formation of PVP-SPAN through partial inhibited galvanic replacement and following etching process was suggested in schematic illustration. (b) At relatively low temperature of 4 and 20 °C, rough morphological nanoparticles were formed, whereas higher temperature induced the formation of smooth and clean surfaced hollow nanoshells (b, top). Through the hydrogen peroxide etching process, rough morphological nanoparticles transformed into spherically-clustered nanoparticles from the particles prepared at low temperatures whereas hollow nanoshell and networked nanoshell were formed from the particles prepared at higher temperature (b, bottom).

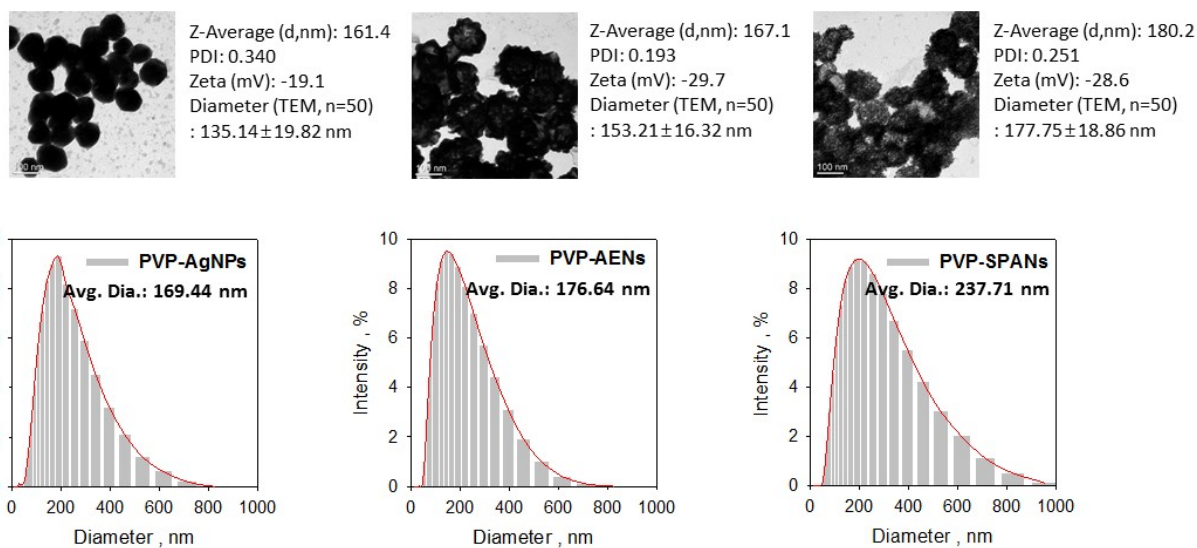


**Figure S2.** TEM, DLS and zeta potential measurement of the synthesized PVP-AgNP, PVP-AEN and PVP-SPAN. All three nanoparticles exhibited strongly negative zeta potential of -19.1 (PVP-AgNP), -29.7 (PVP-AEN) and -28.6 mV (PVP-SPAN) in pH 7.4 solution. The average diameter of the nanoparticles measured based on TEM images (n=50) was 135.14 nm (PVP-AgNP), 153.21 nm (PVP-AEN) and 177.75 nm (PVP-SPAN). The hydrodynamic diameters obtained from the DLS measurement of 176.64 nm (PVP-AgNP), 169.44 nm (PVP-AEN) and 237.71 nm (PVP-SPAN) were larger than those obtained from TEM images.

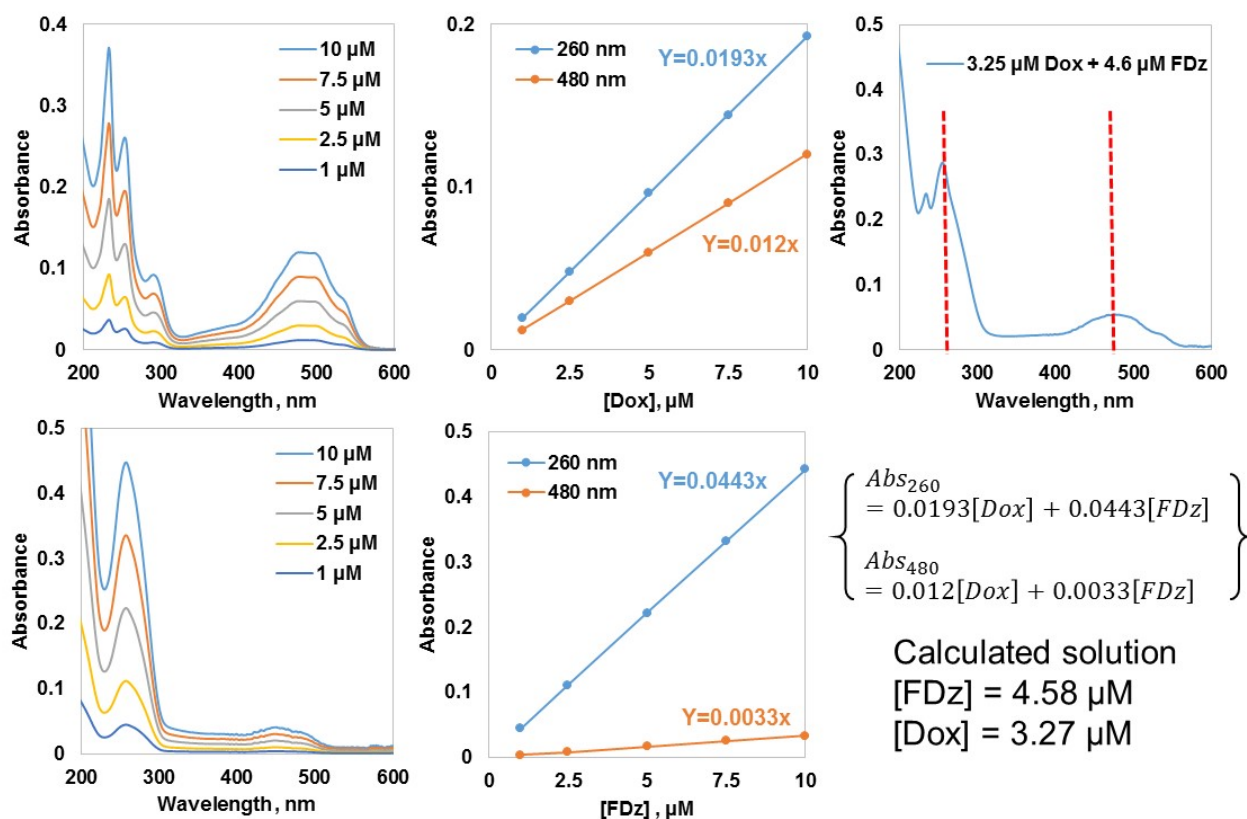


**Figure S3.** Standard UV-Vis spectra obtained at various concentrations of doxorubicin (top) and FDz (bottom). By using the measured spectra, linear plotting of absorbance against concentration was done with linear regression equation. Because the absorbance of Dox and FDz were overlapped, to calculate the exact concentration, we used two equations to solve the concentration. For the final verification, UV-Vis spectra of randomly mixed solution (3.25  $\mu\text{M}$  Dox + 4.6  $\mu\text{M}$  FDz) were prepared and its absorbance was measured. According to the built equation with calculated coefficient, 3.27  $\mu\text{M}$  Dox and 4.58  $\mu\text{M}$  FDz was obtained. These values are well fitted in <0.5% error range.

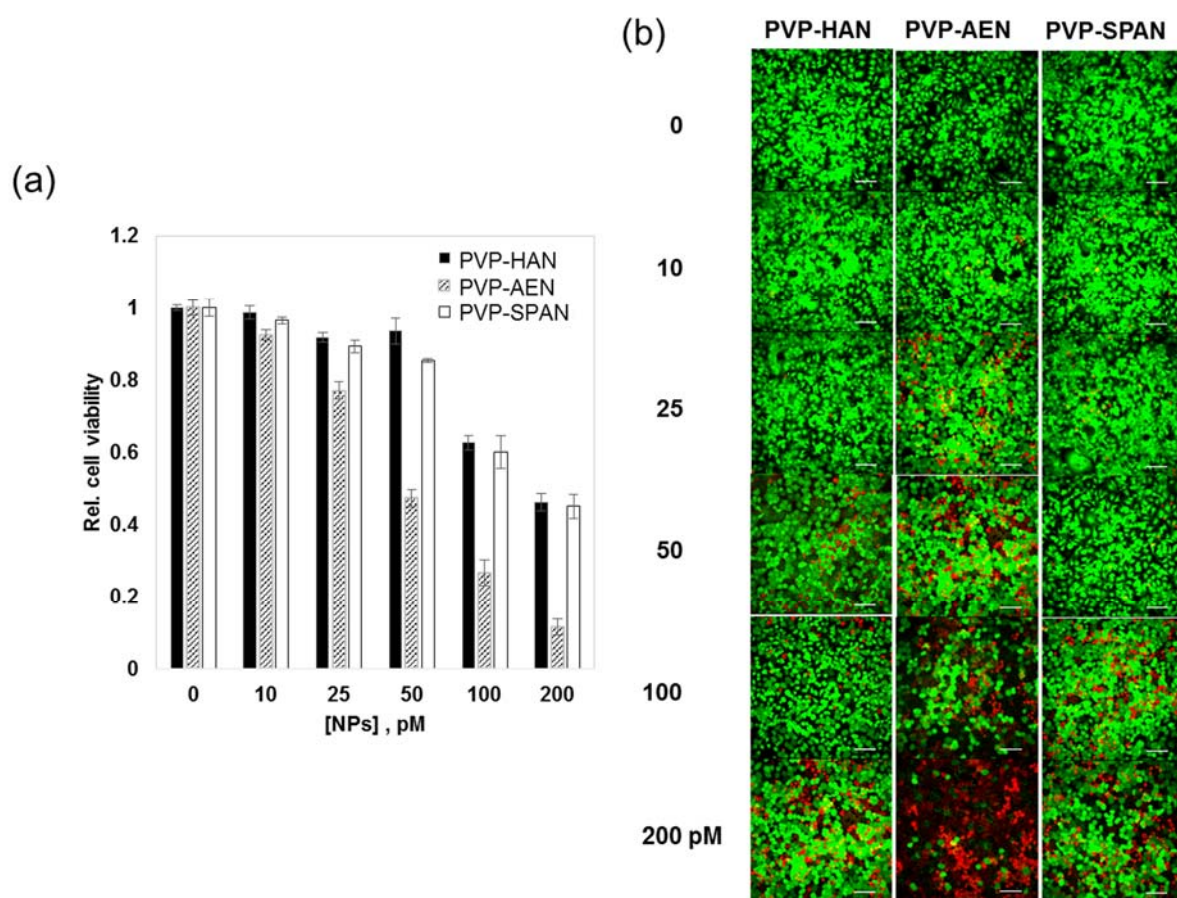


**Figure S4.** Cytotoxicity of PVP-HAN, PVP-AEN and PVP-SPAN measured using NS3 replicon Huh7 cell line. a) According to MTT cell viability assay, PVP HAN and PVP-SPAN exhibited much lower cytotoxicity than PVP-AEN. This tendency may be originated from the possibility of toxic Ag ion dissolution from the PVP-AEN due to omitting etching process. b) Fluorescence microscopy images of the cells after live/dead staining supported the MTT cell viability assay data.